

# Formula for the asymmetric diffraction peak profiles based on double Soller slit geometry

Takashi Ida

*Department of Material Science, Faculty of Science, Himeji Institute of Technology, Kanaji, Kamigori-cho, Ako-gun, Hyogo 678-1297, Japan*

(Received 20 January 1998; accepted for publication 6 March 1998)

The asymmetric diffraction peak profiles and peak shift of conventional powder diffractometry systems caused by the angular divergence along the vertical axis are reproduced by asymmetrized peak profile functions. The asymmetrization is achieved by convoluting the angular dispersions of both incident and scattered beams along the vertical axis. A general method for mapping vertical window functions to the horizontal direction is proposed, and the formulas of two types of horizontal window functions mapped from symmetric double vertical Bartlett (triangular) and Gaussian window functions are presented. Both formulas incorporate a single asymmetry parameter connected with the open width of the Soller slits along the vertical direction. When experimental diffraction peak profiles are fitted by asymmetrized pseudo-Voigt functions, the asymmetry parameter gives good coincidence with the Soller slit angle, which is clearly specified in a given diffractometer. © 1998 American Institute of Physics. [S0034-6748(98)00806-5]

## I. INTRODUCTION

It is generally accepted that the experimental diffraction peak profiles are the convolution of the wavelength spectrum with various functions arising from instrumental factors and specimen defects.<sup>1</sup> In powder diffractometry with large vertical divergence, the diffraction peaks are shifted from their original positions and peak profiles become asymmetric. Rietveld has introduced a "semiempirical" asymmetry factor intended to correct peak shapes for this effect.<sup>2</sup> Howard has proposed an approximation of asymmetric diffraction peaks by a sum of Gaussians which incorporates a single asymmetry parameter.<sup>3</sup> The Howard method is based on a convolution of a Gaussian profile with a rectangular window profile along the vertical direction. However, the assumed geometry does not match the double Soller slit geometry shown in Fig. 1, which is commonly adopted in commercial powder x-ray diffractometry systems with divergent beam sources.

Although considerable improvements in analysis of neutron or synchrotron diffractometry have recently been achieved,<sup>4</sup> mathematically clear formalism applicable to the double Soller slit geometry of conventional powder x-ray diffractometers has not yet been reported to the author's knowledge. Considering the rapid development of computers and computing methods, it is worth establishing a precise mathematical model for commonly used diffractometry systems, even if the exact form might need more computation time than approximated ones.

In this article, the author presents mathematical models for diffraction peak profile asymmetrized by vertical divergence of both incident and scattered beams limited by double Soller slit geometry, and an example of fitting to experimental diffraction peak profiles.

## II. MODEL FUNCTIONS

### A. General procedure for mapping vertical window functions to horizontal direction

Figure 2 illustrates the general geometry of powder diffractometry including vertical divergence. Here  $\alpha$  and  $\beta$  are, respectively, the angles of the deviations of the incident and scattered beams from the horizontal plane. The diffraction angle  $2\theta_0$  for given  $\alpha$  and  $\beta$  is exactly related to the horizontal angle  $2\theta$  by the following equation:

$$\cos 2\theta_0 = \cos 2\theta \cos \alpha \cos \beta + \sin \alpha \sin \beta \quad (1)$$

or

$$2\theta - 2\theta_0 = \arccos(\cos 2\theta_0 \sec \alpha \sec \beta - \tan \alpha \tan \beta) - 2\theta_0 \equiv z(\alpha, \beta). \quad (2)$$

The function  $z(\alpha, \beta)$  can be approximated by

$$z(\alpha, \beta) \cong -\frac{\alpha^2 + \beta^2}{2} \cot 2\theta_0 + \alpha \beta \operatorname{cosec} 2\theta_0, \quad (3)$$

on the assumption that  $\alpha$  and  $\beta$  are sufficiently small. By changing the variables  $(\alpha, \beta)$  to  $(x, y)$  by  $\alpha \equiv (x+y)/\sqrt{2}$  and  $\beta \equiv (x-y)/\sqrt{2}$ , the above relation can be simplified as

$$z \cong -\frac{1}{2} (x^2 - y^2/t), \quad (4)$$

where  $t \equiv \tan \theta_0$ .

We assume that the vertical window profiles of the incident and scattered beams to be  $f_{V1}(\alpha)$  and  $f_{V2}(\beta)$ , and the horizontal profile to be  $f_H(2\Theta - 2\theta)$ , where  $2\Theta$  is the horizontal angle which defines the position of the receiving slit or the detector. When we define  $\Delta 2\theta \equiv 2\Theta - 2\theta_0$ , the convoluted profile function  $P(\Delta 2\theta)$  has a general form of

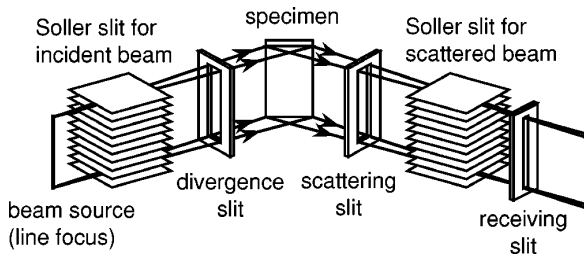


FIG. 1. Schematic view of a conventional powder diffractometry system with double Soller slit geometry.

$$P(\Delta 2\theta) = \int \int \int f_H(2\Theta - 2\theta - 2\theta_0 - z) f_{V1}(\alpha) f_{V2}(\beta) \delta(2\theta - 2\theta_0 - z) d\alpha d\beta d(2\theta), \quad (5)$$

where  $\delta(x)$  is the Dirac delta function. The integration of Eq. (5) on  $2\theta$  gives

$$P(\Delta 2\theta) = \int \int f_H(\Delta 2\theta - z) f_{V1}(\alpha) f_{V2}(\beta) d\alpha d\beta. \quad (6)$$

When we compare the above formula with the following standard form of convolution:

$$P(\Delta 2\theta) = \int f_H(\Delta 2\theta - z) w(z) dz, \quad (7)$$

where  $w(z)$  is the window function to be convoluted to the original profile function  $f_H(z)$ ,  $w(z)$  is found to be given by the following integration:

$$w(z) = \int f_{V1}(\alpha) f_{V2}(\beta) \frac{d\beta}{dz} d\alpha, \quad (8)$$

or alternatively,

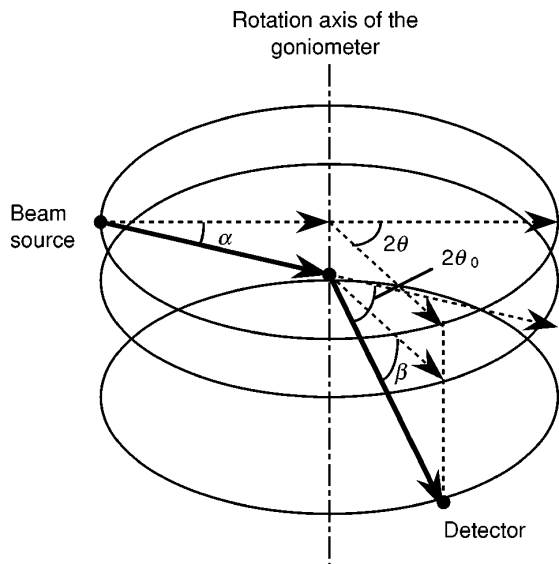


FIG. 2. Geometry of powder diffractometry including vertical divergence. The overall diffraction angle and its horizontal component are denoted by  $2\theta_0$  and  $2\theta$ .  $\alpha$  and  $\beta$  are the angles of the deviations of the incident and scattered beams from the horizontal plane.

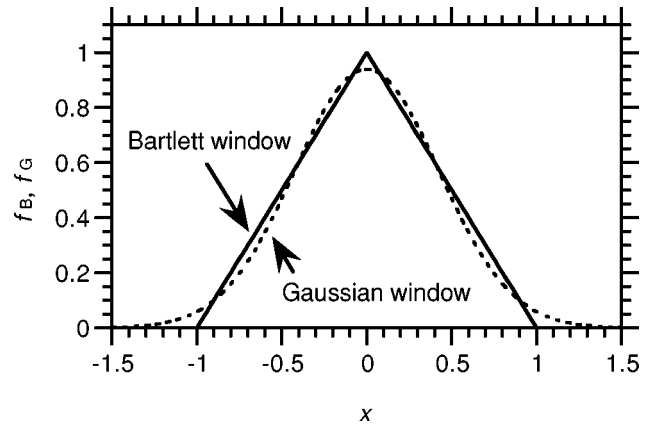


FIG. 3. Profiles of normalized Bartlett and Gaussian window functions with FWHM ( $\Phi_B, \Phi_G$ ) of 1.

$$w(z) = \int f_{V1}\left(\frac{x+y}{\sqrt{2}}\right) f_{V2}\left(\frac{x-y}{\sqrt{2}}\right) \frac{dy}{dz} dx. \quad (9)$$

### B. Mapping of vertical Bartlett windows to the horizontal direction

If the Soller slits are ideally designed and the beam source or the detector have sufficient length in the vertical direction, the vertical window functions should have the profile of a triangle as illustrated in Fig. 3, which is known as a Bartlett window in the field of time series analysis.<sup>5</sup> The normalized Bartlett window function  $f_B(\varphi)$  with the full width at half maximum (FWHM) of  $\Phi_B$  is given by

$$f_B(\varphi) = \frac{1}{\Phi_B} \left(1 - \frac{|\varphi|}{\Phi_B}\right) \text{ for } |\varphi| < \Phi_B, \quad (10)$$

and  $f_B(\varphi) = 0$ , elsewhere. Usually the Soller slits for the incident and scattered beams have symmetric geometry, that is,

$$f_{V1}(\varphi) = f_{V2}(\varphi) = f_B(\varphi). \quad (11)$$

The horizontal window function  $w_{BB}(z)$  mapped from Eqs. (4), (10), and (11) is derived by solving the integration in Eq. (9). In case  $t \leq 1$  ( $2\theta_0 < 90^\circ$ ), the analytical solution of  $w_{BB}$  has the following forms:

$$\frac{\Phi_B^2}{4} w_{BB} = - \frac{(1+t^2 u)[3t + \sqrt{1-(1-t^2)u}]}{2(1+t\sqrt{1-(1-t^2)u})} + \left(1 - \frac{1+t^2}{2} u\right) \ln \frac{1 + \sqrt{1-(1-t^2)u}}{(1+t)\sqrt{-u}}$$

$$\text{for } -\frac{1}{t^2} \leq u \leq -\frac{1-t^2}{4t^2}, \quad (12)$$

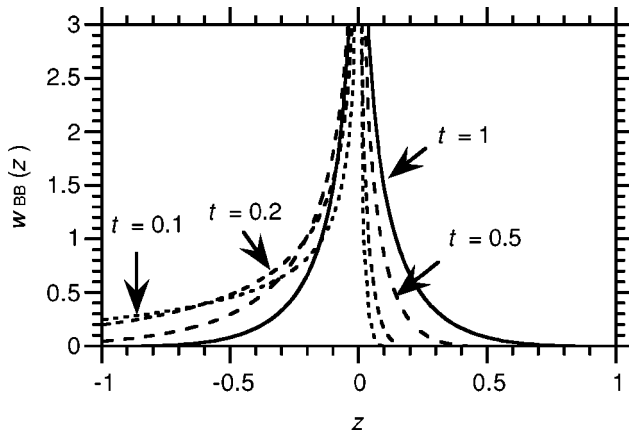


FIG. 4. Horizontal window function  $w_{BB}$  mapped from symmetric double vertical Bartlett window functions with the FWHM  $\Phi_B=1$  for various  $t$  ( $=\tan\theta_0$ ) values.

$$\frac{\Phi_B^2}{4} w_{BB} = -\frac{(1+t^2 u)[3t + \sqrt{1-(1-t^2)u}]}{2(1+t\sqrt{1-(1-t^2)u})} + t u + 2\sqrt{-(1-t^2)u} + \left(1 + \frac{1+t^2}{2}u\right) \times \ln \frac{1 + \sqrt{1-(1-t^2)u}}{(1+t)\sqrt{-u}} + \frac{1+t^2}{2} u \ln \frac{1-t}{1+t}$$

for  $-\frac{1-t^2}{4t^2} \leq u < 0$ ,

$$\frac{\Phi_B^2}{4} w_{BB} = -\frac{(1+t^2 u)[3t + \sqrt{1-(1-t^2)u}]}{2(1+t\sqrt{1-(1-t^2)u})} + \left(1 + \frac{1+t^2}{2}u\right) \ln \frac{1 + \sqrt{1-(1-t^2)u}}{(1+t)\sqrt{u}}$$

for  $0 < u \leq 1$ ,

where

$$u \equiv \frac{z}{\Phi_B^2 t}.$$

In case  $t > 1$ ,  $w_{BB}$  can be derived from the above form and the following relation:

$$w_{BB}(z, t) = w_{BB}\left(-z, \frac{1}{t}\right).$$

Figure 4 plots the profiles of the  $w_{BB}(z)$  function for various  $t$  values. It should be noted that  $w_{BB}(z)$  has finite width at  $t=1$ , which means that the vertical divergence in conventional diffractometry system contributes to the width of the convoluted diffraction peak, even if  $t=1$ .

### C. Mapping of vertical Gaussian windows to the horizontal direction

Although the geometry of Soller slits is naturally modeled by the double vertical Bartlett windows discussed in the preceding section, we here examine the formula for mapping

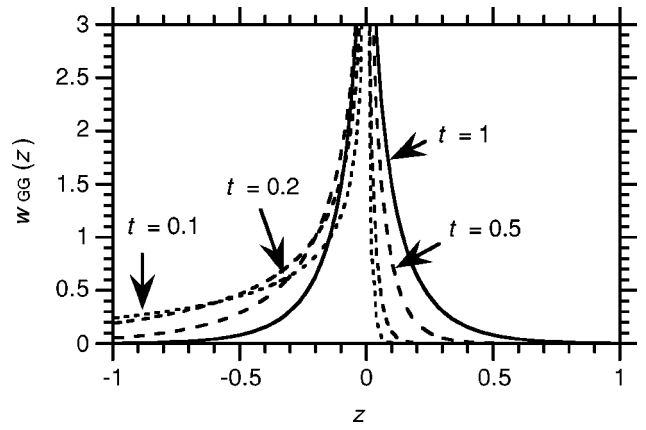


FIG. 5. Horizontal window function  $w_{GG}$  mapped from symmetric double vertical Gaussian window functions with the FWHM  $\Phi_G=1$  for various  $t$  ( $=\tan\theta_0$ ) values.

vertical Gaussian windows, the analytical solution of which is easier owing to the infinite integral range. Furthermore, a model based on Gaussian windows will be appropriate, if the real Soller slits have random error in geometry. The normalized Gaussian window function  $f_G(\varphi)$  with the FWHM of  $\Phi_G$  is given by

$$f_G(\varphi) = \frac{2\sqrt{\ln 2}}{\sqrt{\pi} \Phi_G} \exp\left[-4(\ln 2) \frac{\varphi^2}{\Phi_G^2}\right] \quad (17)$$

or

$$f_G(\varphi) = \frac{1}{\sqrt{\pi} \Psi_G} \exp\left[-\frac{\varphi^2}{\Psi_G^2}\right], \quad (18)$$

where

$$\Psi_G \equiv \frac{\Phi_G}{2\sqrt{\ln 2}}.$$

The profile of  $f_G(\varphi)$  is illustrated in Fig. 3. When the Soller slits for the incident and scattered beams have symmetric geometry again,

$$f_{v1}(\varphi) = f_{v2}(\varphi) = f_G(\varphi).$$

The horizontal window function  $w_{GG}$  mapped by Eqs. (4) and (9) has a much more simple analytical form than  $w_{BB}$ , that is,

$$w_{GG} = \frac{2}{\pi \Psi_G^2} \exp\left[\frac{t^2-1}{t} \frac{z}{\Psi_G^2}\right] K_0\left(\frac{t^2+1}{t} \frac{|z|}{\Psi_G^2}\right), \quad (21)$$

where  $K_0(x)$  is the modified Bessel function of the second kind. Figure 5 plots the profiles of the  $w_{GG}(z)$  function for various  $t$  values. The profile of  $w_{GG}(z)$  is found to be quite similar to that of  $w_{BB}(z)$  shown in Fig. 4, while the analytical forms are considerably different.

### III. APPLICATION TO FIT EXPERIMENTAL PEAK PROFILES

In this section, the above models for powder diffraction profiles are tested by fitting to experimental powder x-ray diffraction data. Experimental diffraction profiles of Si were

TABLE I. Fitting parameters for Si diffraction data on the model based on symmetric double vertical Bartlett (triangular) windows.

| <i>hkl</i> | $2\theta_0$ (deg) | $\Gamma_G$ (deg) | $\Gamma_L$ (deg) | $\Phi_B$ (deg) | <i>f</i> | <i>f</i> <sub>0</sub> | <i>R</i> <sub>P</sub> (%) |
|------------|-------------------|------------------|------------------|----------------|----------|-----------------------|---------------------------|
| 111        | 28.435            | 0.043            | 0.019            | 2.38           | 1276     | 60                    | 5.2                       |
| 220        | 47.296            | 0.044            | 0.023            | 2.61           | 613      | 33                    | 3.3                       |
| 311        | 56.113            | 0.048            | 0.025            | 2.58           | 446      | 26                    | 3.1                       |
| 400        | 69.115            | 0.052            | 0.026            | 2.93           | 112      | 12                    | 3.3                       |
| 331        | 76.366            | 0.047            | 0.026            | 2.97           | 216      | 19                    | 2.9                       |
| 422        | 88.011            | 0.051            | 0.045            | 2.68           | 191      | 19                    | 2.6                       |
| 333        | 94.930            | 0.046            | 0.046            | 2.78           | 163      | 15                    | 2.3                       |
| 440        | 106.684           | 0.042            | 0.059            | 2.81           | 82       | 14                    | 3.0                       |
| 531        | 114.067           | 0.044            | 0.072            | 2.52           | 191      | 14                    | 2.6                       |
| 620        | 127.509           | 0.039            | 0.086            | 2.89           | 190      | 17                    | 2.6                       |
| 533        | 136.857           | 0.048            | 0.100            | 2.88           | 106      | 18                    | 3.2                       |

collected with a commercial powder x-ray diffractometer, Rigaku RINT-2000, with a Cu *K* $\alpha$  radiation tube as the x-ray source. The radius of the goniometer circle is 185 mm, and 0.15 mm width receiving slit, 1°-open divergence and scattering slits were used. The specified Soller slit angle 5° is identified with twice the FWHM of the vertical window functions. No corrections of the instrumental error were applied. The overall profile function is calculated by numerical integration of Eq. (7), assuming that the horizontal profile is expressed by a pseudo-Voigt function,<sup>6,7</sup>

$$f_H(x) = (1 - \eta) \frac{2\sqrt{\ln 2}}{\sqrt{\pi} \Gamma} \exp\left[-4(\ln 2)\left(\frac{x}{\Gamma}\right)^2\right] + \eta \frac{2}{\pi \Gamma} \left[1 + 4\left(\frac{x}{\Gamma}\right)^2\right]^{-1}, \quad (22)$$

$$\eta = 1.36603 \frac{\Gamma_L}{\Gamma} - 0.47719 \left(\frac{\Gamma_L}{\Gamma}\right)^2 + 0.11116 \left(\frac{\Gamma_L}{\Gamma}\right)^3, \quad (23)$$

$$\Gamma = (\Gamma_G^5 + 2.69269 \Gamma_G^4 \Gamma_L + 2.42843 \Gamma_G^3 \Gamma_L^2 + 4.47163 \Gamma_G^2 \Gamma_L^3 + 0.07842 \Gamma_G \Gamma_L^4 + \Gamma_L^5)^{1/5}, \quad (24)$$

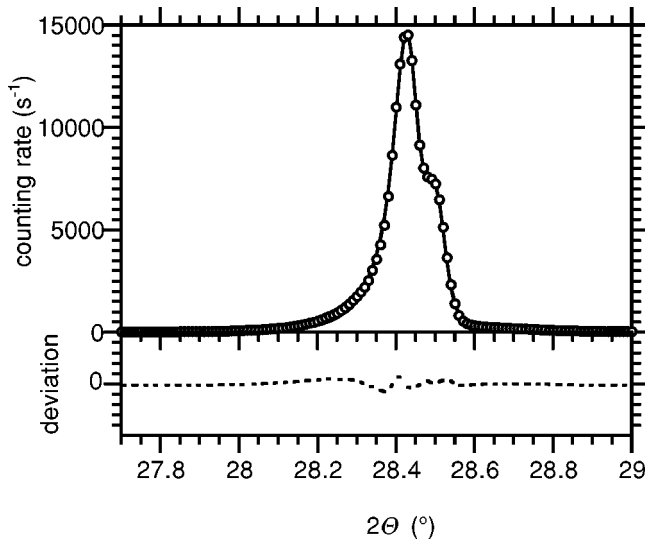


FIG. 6. Experimental (open circles) and calculated (solid line) peak profiles and error plot (dotted line) for Si 111-reflection. Calculation is based on the geometry of double vertical Bartlett (triangular) windows.

TABLE II. Fitting parameters for Si diffraction data on the model based on symmetric double vertical Gaussian windows.

| <i>hkl</i> | $2\theta_0$ (deg) | $\Gamma_G$ (deg) | $\Gamma_L$ (deg) | $\Phi_G$ (deg) | <i>f</i> | <i>f</i> <sub>0</sub> | <i>R</i> <sub>P</sub> (%) |
|------------|-------------------|------------------|------------------|----------------|----------|-----------------------|---------------------------|
| 111        | 28.435            | 0.043            | 0.019            | 2.36           | 1287     | 46                    | 4.2                       |
| 220        | 47.296            | 0.045            | 0.023            | 2.56           | 616      | 29                    | 3.0                       |
| 311        | 56.113            | 0.049            | 0.025            | 2.54           | 447      | 24                    | 3.0                       |
| 400        | 69.115            | 0.054            | 0.024            | 2.94           | 112      | 12                    | 3.4                       |
| 331        | 76.366            | 0.050            | 0.023            | 3.03           | 215      | 19                    | 3.0                       |
| 422        | 88.011            | 0.053            | 0.041            | 2.82           | 189      | 20                    | 2.6                       |
| 333        | 94.930            | 0.049            | 0.045            | 2.74           | 163      | 14                    | 2.3                       |
| 440        | 106.684           | 0.045            | 0.057            | 2.81           | 82       | 14                    | 2.9                       |
| 531        | 114.067           | 0.046            | 0.071            | 2.44           | 191      | 14                    | 2.5                       |
| 620        | 127.509           | 0.043            | 0.085            | 2.84           | 191      | 16                    | 2.6                       |
| 533        | 136.857           | 0.050            | 0.100            | 2.80           | 106      | 17                    | 3.3                       |

where  $\Gamma_G$  and  $\Gamma_L$  are Gaussian and Lorentzian FWHMs. Two types of window functions,  $w_{BB}(z)$  defined by Eqs. (12)–(15) and  $w_{GG}(z)$  defined by Eq. (21) are examined. The position and the integrated intensity of the *K* $\alpha_1$  peak ( $2\theta_0, f$ ), Gaussian and Lorentzian FWHMs ( $\Gamma_G, \Gamma_L$ ), constant background *f*<sub>0</sub>, and the FWHM of the Soller slits  $\Phi_B$  or  $\Phi_G$  are treated as independent adjustable parameters for each peak. The results of the least-squares fit to 111-533 reflections are listed in Tables I and II. The *R* factor for the profile fitting *R*<sub>P</sub> defined by

$$R_P = \sum_i |Y(2\theta_i)_{obs} - Y(2\theta_i)_{calc}| / \sum_i Y(2\theta_i)_{obs}, \quad (25)$$

where  $Y(2\theta_i)_{obs}$  and  $Y(2\theta_i)_{calc}$  are, respectively, observed and calculated data, are listed in the last columns of the tables. Figures 6 and 7 show the experimental Si 111-reflection data, the best fit curves and the deviations. The observed asymmetry of the peak is well reproduced by the model functions. Practically no significant difference has been found in the best fit curve or estimated parameters between models based on Bartlett and Gaussian window functions. The estimated FWHM values of the Soller slits  $\Phi_B$  and  $\Phi_G$  are close to 2.5° for all reflection peaks, which can be

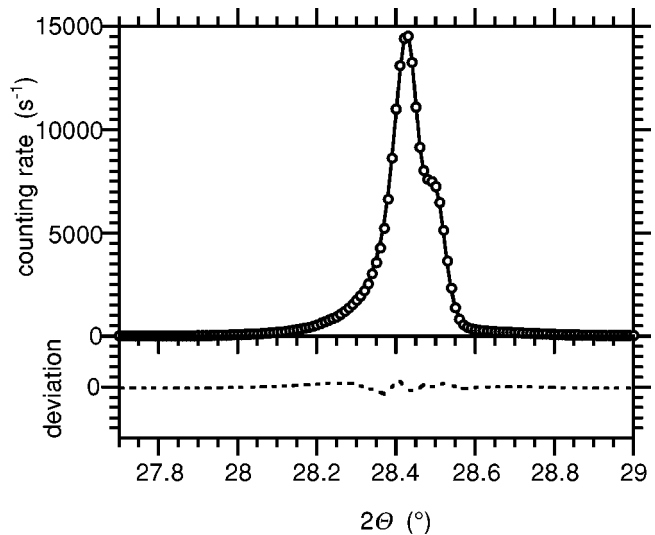


FIG. 7. Experimental (open circles) and calculated (solid line) peak profiles and error plot (dotted line) for Si 111-reflection. Calculation is based on the geometry of double vertical Gaussian windows.

identified with half of the specified Soller slit open angle. The estimated FWHM of the horizontal Gaussian component  $\Gamma_G$  is close to the value  $0.046^\circ$  which is the arctangent of the ratio of the receiving slit width to goniometer radius. It should be noted that the iteration steps in the curve fitting procedure normally converged in all cases, and the final values of  $\Phi_B$  and  $\Phi_G$  are plausible, even if  $2\theta_0$  is near  $90^\circ$  and the profile is almost symmetric, which supports that not only the asymmetry but also the symmetric feature of the convoluted profile is considerably affected by the vertical divergence. Simultaneous estimation of  $\Gamma_G$ ,  $\Gamma_L$  and  $\Phi_B$  or  $\Phi_G$  for each peak seems to have uncertainty due to the mutual correlations. However, these uncertainties are expected to be avoided in a Rietveld analysis, when the angular dependences of  $\Gamma_G$  and  $\Gamma_L$  are properly modeled and a constant

value for  $\Phi_B$  or  $\Phi_G$  is assumed. Since  $\Phi_B$  or  $\Phi_G$  is a purely instrumental factor, the value can be fixed, if the geometry of the Soller slits of a given diffractometer is once precisely specified.

- <sup>1</sup>J. I. Langford, *J. Appl. Crystallogr.* **11**, 10 (1978).
- <sup>2</sup>H. M. Rietveld, *J. Appl. Crystallogr.* **2**, 65 (1969).
- <sup>3</sup>C. J. Howard, *J. Appl. Crystallogr.* **15**, 615 (1982).
- <sup>4</sup>L. W. Finger, D. E. Cox, and A. P. Jephcoat, *J. Appl. Crystallogr.* **27**, 892 (1994).
- <sup>5</sup>W. H. Press, B. P. Flannery, S. A. Teukolsky, and W. T. Vetterling, *Numerical Recipes* (Cambridge University Press, Cambridge, 1986), Chap. 12.
- <sup>6</sup>G. K. Wertheim, M. A. Butler, K. W. West, and D. N. E. Buchanan, *Rev. Sci. Instrum.* **45**, 1369 (1974).
- <sup>7</sup>P. Thompson, D. E. Cox, and J. B. Hastings, *J. Appl. Crystallogr.* **20**, 79 (1987).